

Surface Structure and Electron Density Dependence of Scattered Ne^+ Ion Fractions from Cd- and S-Terminated $\text{CdS}\{0001\}$ Surfaces

L. Houssiau and J. W. Rabalais

Department of Chemistry, University of Houston, Houston, Texas 77204-5641

J. Wolfgang and P. Nordlander

Department of Physics and Rice Quantum Institute, Rice University, Houston, Texas 77251

(Received 29 June 1998)

Experimental measurements of the magnitudes and azimuthal anisotropies of 4 keV Ne^+ scattered ion fractions from both the Cd- and S-terminated surfaces of $\text{CdS}\{0001\}$ exhibit high sensitivity to both surface structure and electron density. Using a density functional approach, a clear correlation has been demonstrated between these Ne^+ ion fractions and the lateral variation of the electrostatic potential along the outgoing trajectories of the scattered Ne atoms. The observed anisotropy in the ion fractions is a result of the variations in surface to atom electron transfer rates due to tunneling barriers introduced by the electrostatic potentials. [S0031-9007(98)07848-X]

PACS numbers: 61.80.Ba, 61.80.Jh, 71.20.Nr, 79.20.Rf

Electron charge transfer processes play a fundamental role in many dynamical phenomena at surfaces [1–3]. The interactions of atoms and molecules with metal surfaces are relatively well understood. Methods have been developed for calculation of the energy shifts and broadening of atomic and molecular levels near these surfaces [4,5] and for the description of dynamical interactions in atom-surface scattering experiments [6,7]. A general understanding is beginning to emerge [8] for more complicated charge transfer processes such as Auger neutralization and deexcitation.

For semiconductors and insulators, the situation is less well understood. No general understanding [9] of the neutralization and deexcitation channels has emerged. An experimental and theoretical investigation of the neutralization probabilities of Ne^+ ions scattered from both the Cd- and S-terminated surfaces of $\text{CdS}\{0001\}$ are presented herein. The electronic properties of the surface which influence ion neutralization have been identified. A pronounced sensitivity of the neutralization probability of Ne^+ to surface structure and electron density is revealed. The neutralization probability correlates with the variations of the local electrostatic potential on these surfaces as calculated from a density functional approach. This may provide the basis for the further development of a general theory for charge transfer reactions on semiconductors and insulators.

The measurements were carried out in a time-of-flight scattering and recoiling spectrometer (TOF-SARS) [10]. The technique uses a pulsed noble gas ion beam which is scattered from a sample surface in a UHV chamber. The scattered and recoiled ions plus fast neutrals are measured by TOF techniques. A 4 keV Ne^+ ion beam with a pulse width of ~ 50 ns, pulse rate of 30 kHz, and average ion current of ~ 0.5 nA/cm² was used. Ion fraction measurements were made by using a 50 cm long acceleration tube located within the 90 cm sample to detector drift region.

Ions are accelerated by the electric field, thereby separating the ion and neutral fractions. The acceleration tube acts as a lens which focuses the ions onto the detector. The absolute values of the ion fractions [11] are obtained by correcting for this focusing factor by grounding the tube and using a set of deflection plates which deflect all of the ions out of the scattered flux such that only the neutrals are detected. The difference in the number of particles measured with no voltage on the deflection plates (neutrals + ions) and with a voltage (only neutrals) gives the absolute number of ions. The detection efficiencies of keV neutrals and ions are similar [11].

CdS has a wurtzite structure which gives rise to a crystallographic polarity; i.e., it is terminated in either a Cd or a S layer. Because of the inversion plane, experiments on both the $\{0001\}$ Cd-terminated and the $\{000\bar{1}\}$ S-terminated surfaces could be made on a single sample by rotating the crystal. Measurements were made on three different samples which were cleaned in UHV by several cycles of 500 eV Ar^+ sputtering ($0.5 \mu\text{A}/\text{cm}^2$ for 10 min) followed by annealing at $\sim 700^\circ\text{C}$ for 10 min. Both surfaces exhibited a (1×1) LEED pattern, although considerable differences in the brightness was observed. For the Cd termination, a sharp pattern was obtained after only two or three cycles of sputtering and annealing. For the S termination, the pattern remained faint, even after repeated sputtering cycles or longer annealing times as we have recently reported [12]. Both surfaces are unreconstructed and contain two different coexisting domains, rotated by 60° from each other [12]. This results in a 60° azimuthal periodicity of the TOF-SARS scans, rather than the 120° periodicity expected for a single domain.

Spectra of 4 keV Ne^+ scattering from the $\text{CdS}\{0001\}$ and $\{000\bar{1}\}$ surfaces both with and without the acceleration voltages are shown in Fig. 1. Without the acceleration voltages, both surfaces exhibit an intense peak at $\sim 4.8 \mu\text{s}$ due to Ne scattering from Cd [$\text{Ne}(\text{s})/\text{Cd}$] and a weaker

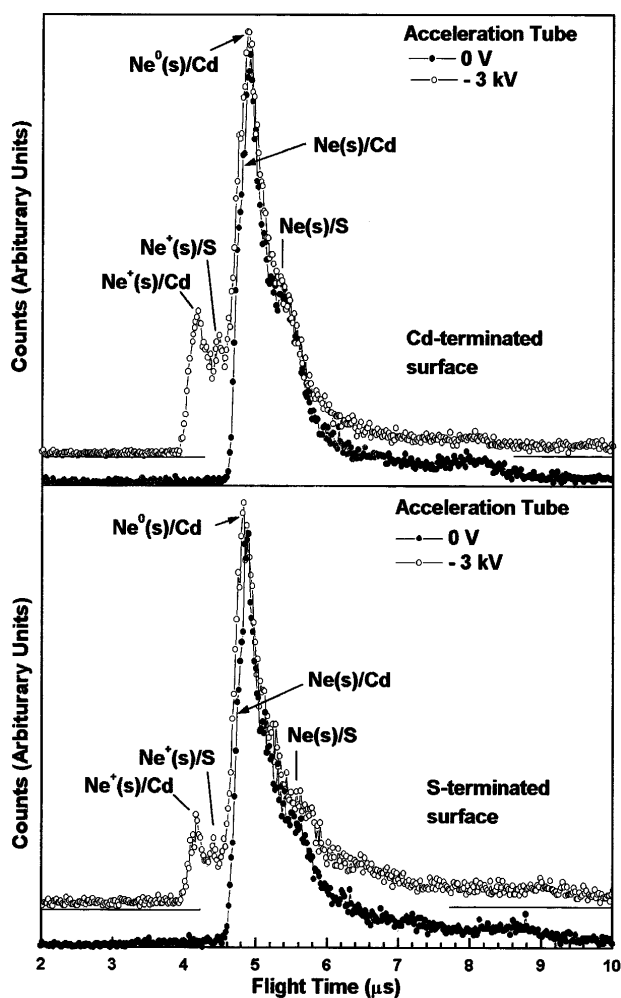


FIG. 1. TOF-SARS spectra of Ar^+ impinging on the Cd- and S-terminated surfaces of CdS. Solid circles: neutral plus ion spectrum. Open circles: ion accelerated spectrum.

broad peak due to Ne scattering from S [$\text{Ne}(s)/\text{S}$] at $\sim 5.4 \mu\text{s}$. Upon application of -3 kV to the acceleration tube, the Ne^+ ions are accelerated, separating the $\text{Ne}(s)/\text{Cd}$ peak into its neutral $\text{Ne}^0(s)/\text{Cd}$ (unshifted) and ionic $\text{Ne}^+(s)/\text{Cd}$ (shifted to $\sim 4.2 \mu\text{s}$) components and the $\text{Ne}(s)/\text{S}$ peak into its neutral $\text{Ne}^0(s)/\text{S}$ (unshifted) and ionic $\text{Ne}^+(s)/\text{S}$ (shifted to $\sim 4.6 \mu\text{s}$) components. The spectra from both surfaces are similar, with the exception of the different intensities of the $\text{Ne}^+(s)/\text{Cd}$ peaks. The $\text{Ne}^+(s)/\text{Cd}$ peak is more intense than expected due to the focusing factor of the tube. The actual Ne^+ ion fractions for the Cd- and S-terminated surfaces average $\sim 5.7\%$ and $\sim 4.2\%$, respectively.

These scattered Ne^+ ion fractions were highly sensitive to the alignment of the ion beam with the crystal azimuthal directions. Azimuthal scans of the ion fractions were obtained by rotating the crystal about its normal and acquiring TOF spectra at 2° intervals. The ion fractions were calculated [13] as the ratio of intensities $\text{Ne}^+ / (\text{Ne}^0 + \text{Ne}^+)$, after correction of the Ne^+ signal for the focusing factor, using the areas of $0.3 \mu\text{s}$ windows centered at the

maxima of the peaks. These ion fractions (Fig. 2) exhibit a periodic behavior as a function of azimuthal angle. They are higher on the Cd- than the S-terminated surface and the maxima and minima have exactly the opposite behavior on these two surfaces.

For the Cd termination, the *lowest* ion fractions are found along the close-packed atomic rows, i.e., along the azimuths 0° ($\langle 100 \rangle$), 60° ($\langle 0\bar{1}00 \rangle$), and 120° ($\langle 0010 \rangle$). The Ne^+ neutralization probability is hence *enhanced*, or, comparably, the ion survival probability is *decreased*, along these dense Cd rows. Minima are also observed along the 30° ($\langle 1\bar{1}00 \rangle$) and 90° ($\langle 0\bar{1}10 \rangle$) azimuths; however, they are not as deep as those along the close-packed directions. The observed periodicity of the oscillations is 30° .

For the S termination, the *highest* ion fractions are found along the principal azimuths, i.e., 0° , 30° , 60° , and 90° , and they exhibit a 30° periodicity. Because of the low incident angle of $\alpha = 11^\circ$, the trajectories of the incident Ne^+ ions are influenced by grazing multiple collisions with 1st-layer S atoms. Analysis of the trajectories using SARIC [14] shows that this is particularly pronounced along the high symmetry azimuths at 0° , 30° , 60° , etc. This is known as quasisingle scattering, where the projectile makes several small angle deflection collisions with S atoms and a single large angle deflection collision with a Cd atom; the latter collision determines the final scattered ion energy. The structure of the CdS surface, with its short 1st-layer S to 2nd-layer Cd spacings (0.84 \AA), long 2nd-layer Cd to 3rd-layer S spacings (2.51 \AA), and short lateral spacings between the 1st-layer S and 2nd-layer Cd (1.19 \AA), emphasizes such multiple scattering collisions. The experiment implies high ion fractions along trajectories close to 1st-layer S atoms. These results demonstrate that the scattered ion fractions are sensitive to both the surface structural corrugation as well as the elemental composition.

First principles calculation of the probability for resonance or Auger charge transfer near a CdS surface is beyond the capabilities of our present methods. Our focus is to identify which properties of the surface will influence the neutralization of atoms near a semiconductor surface such as CdS. Neutralization of the Ne^+ ion can occur through resonant tunneling into the $\text{Ne}(3s)$ level and through Auger deexcitation and neutralization [13]. In all cases, an electron is transferred from the crystal through the surface into the atom. An important factor in determining the neutralization rate is the electrostatic potential barrier introduced by the surface.

The electronic structure of the CdS surface was calculated using a density functional approach [15]. The surface was approximated by using a cluster whose size was increased until the charge density in an interior unit cell did not change with increasing size. The resulting clusters contain up to 74 atoms partitioned in up to four layers (Cd-S-Cd-S-Cd-S-Cd-S).

The calculation shows that the CdS surface is slightly ionic. A Mulliken charge analysis indicates that the surface Cd and S atoms carry net charges of $+0.55$ and -0.55 ,

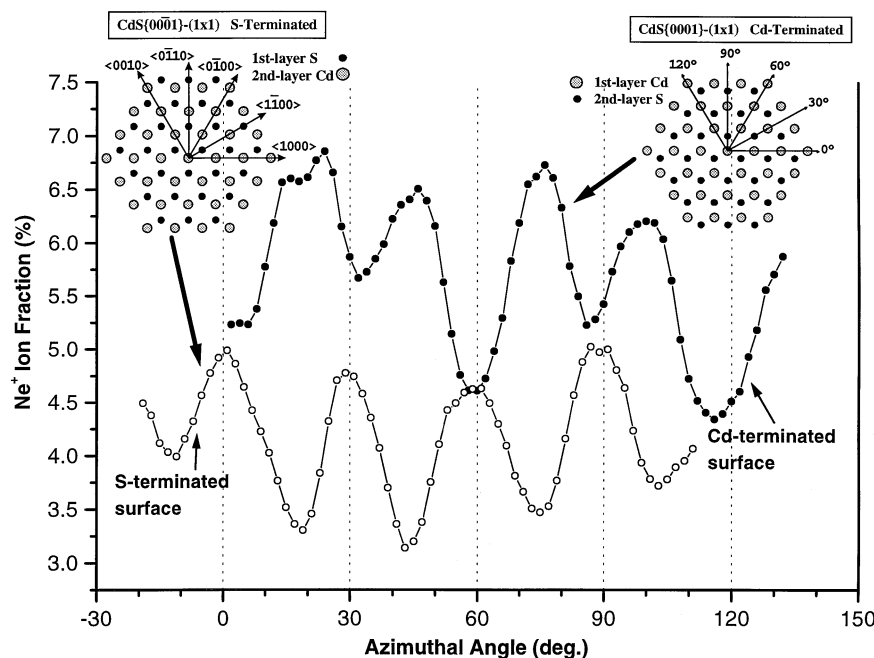


FIG. 2. Scattered Ne^+ ion fractions versus crystal azimuthal angle for the Cd- and S-terminated surfaces. Solid circles: Cd termination. Open circles: S termination.

respectively. This is verified by a calculation of the electrostatic potential along the surface, which is found to be negative near S and positive near Cd atoms. The microscopic origin of the spatial dependence of these electrostatic potentials can be determined by an investigation of the density of states.

The valence orbitals of CdS are composed primarily of the $S(3p)$ and $\text{Cd}(5s)$ atomic states. An investigation of the projected density of states (PDOS) for the CdS cluster allows determination of the spatial distribution of the valence electrons at the surface. For both terminations, the largest contribution to the occupied DOS near the Fermi level comes from the $S(3p)$ states. The calculated PDOS for $\text{Cd}(5s)$ provides a negligible contribution to the occupied DOS near the Fermi level. The accumulation of electronic charge near the S atoms introduces an electrostatic potential energy barrier. Since electron transfer processes must occur through this barrier, the probability of electron transfer is reduced near S atoms. Conversely, the depletion of electronic charge around the Cd atoms lowers the potential energy barrier, thus increasing the electron transfer rates in the vicinity of Cd atoms. This is analogous to the finding [16] of strongly increased (decreased) electron tunneling rates near electropositive (electronegative) impurities on metals.

A qualitative explanation of the periodic charge transfer patterns is obtained from the lateral dependence of the neutralization rates of a Ne^+ ion outside the surface. S-rich paths yield low electron transfer rates and high ion fractions. Cd-rich paths (thus S-poor) yield high electron transfer rates and low ion fractions. For the Cd-termination, after averaging over the two experimental domains (rotated 60° with respect to each other), the Cd-rich rows occur at 0° , 60° , and 120° . This correlates with the deepest minima observed experimentally in Fig. 2. The

30° and 90° directions provide less dense Cd rows, hence lower electron transfer rates, and shallower minima in Fig. 2. In between these Cd-rich rows, at 15° , 45° , 75° , and 105° , the electrostatic potential is repulsive due to the proximity of 2nd-layer S atoms. Exit paths over these regions experience lower neutralization rates than exit paths along the Cd-rich regions, forming the maxima of Fig. 2.

The case is even more apparent for the S termination. Since the 1st-layer S atom dictates the valence charge density, S-rich incident paths along 0° and 60° and S-rich exit paths along 30° and 90° , averaged over the two experimental domains, present repulsive surface potentials, lower electron transfer rates, and higher Ne^+ ion fractions.

At a collision energy of 4 keV and scattering angle of $\theta = 50^\circ$, the impact parameter for Ne^+ scattering from Cd is 0.790 a.u. as calculated from the Ziegler-Biersack-Littmark (ZBL) potential [17]. The positive ions can be neutralized in the close encounter with the Cd atoms or by electron capture along the trajectories. Neutralization during the close encounter can be an efficient process [13]; however, it is not likely to introduce an azimuthal variation of the ion fractions, we neglect the electronic processes occurring during the close encounter. On the contrary, the probabilities of surface to atom electron transfer processes will be sensitive to the incident and exit trajectories.

We assume that neutralization of scattered Ne^+ can be described by a rate equation [18]

$$dn(t)/dt = -\Gamma[\bar{R}(t)]n(t), \quad (1)$$

where $\bar{R}(t)$ is the trajectory of the scattered Ne and $\Gamma[\bar{R}(t)]$ is the instantaneous neutralization rate of Ne^+ at position $\bar{R}(t)$. The electron transfer probabilities $\bar{R}(t)$ will be modulated by the potential barriers caused by the inhomogeneous electrostatic potential near the surface. For simplicity, assume that for the Cd (S) termination, Γ is

enhanced (decreased) by 100% (67%) within a cylindrical region of radius 2.5 a.u. above the Cd (S) atoms. Equation (1) is integrated along the Ne^+ trajectory. In order to model the relatively complicated Ne/S multiple collisions on the S-terminated surface, two simplified trajectories were used. Examples of these trajectories along the $\langle 1000 \rangle$ azimuth are the following: (1) A trajectory with a turning point at 0.79 a.u. above a 2nd-layer Cd atom. (2) A trajectory along $\langle 1000 \rangle$ which is displaced by 4 a.u. in $\langle 0\bar{1}10 \rangle$. The final charge transfer along $\langle 1000 \rangle$ of the S termination is taken as the average charge transfer for these two trajectories. The dependence of the neutralization rate as a function of distance (z) to the surface layer is assumed to be a saturated exponential; i.e., $\Gamma[z] = 0.01$ a.u. for ion-surface distances $z < 3$ a.u. and $\Gamma[z] = 0.01 \exp[-(Z - 3)]$ a.u. for $z \geq 3$ a.u. These parameters have reasonable magnitudes based on previous studies [4,11,13,15]. The essential physics is the prediction of a decreased neutralization probability near S atoms and an increased neutralization probability near Cd atoms.

The calculated ion fractions as a function of azimuthal angle are shown in Fig. 3. The calculation shows larger ion fractions for Ne^+ scattering from the Cd termination than from the S termination, in agreement with experimental results. The reason for this is that for the S termination, the ions emerge from a collision with a 2nd-layer Cd atom so that they travel a larger distance in the surface region and, hence, have a higher neutralization probability. For the Cd termination, the minima along the 0° , 60° , and 120° Cd close-packed directions are due to efficient neutralization above these nearest neighbor Cd atoms. The weaker minima in the 30° and 90° directions are caused by the less efficient neutralization probability above the less dense rows of next nearest neighbor Cd atoms in the surface layer. For the S termination, the situation is reversed due to the decreased electron transfer rates above

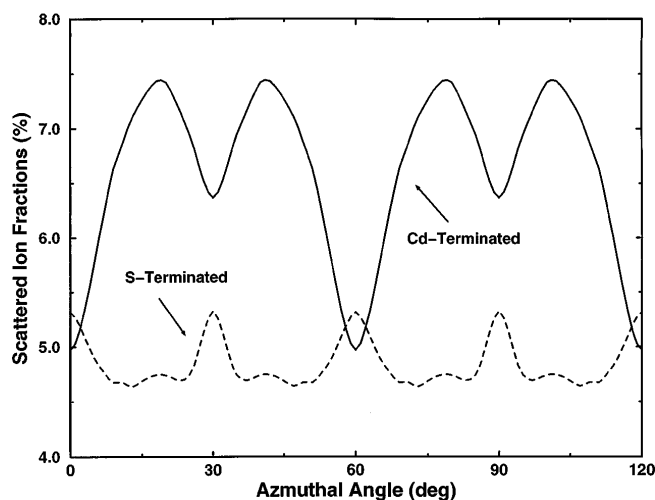


FIG. 3. Calculated azimuthal dependence of the scattered Ne^+ ion fractions. Solid line: Cd termination. Dashed line: S termination.

S atoms. In this case, maxima are calculated for the 0° , 60° , and 120° S close-packed directions. Slightly narrower maxima are calculated along the 30° and 90° directions, which are composed of less dense rows of S atoms.

The magnitudes and azimuthal anisotropies of Ne^+ scattered ion fractions from both the Cd- and S-terminated surfaces of $\text{CdS}\{0001\}$ are highly sensitive to both surface structure and electron density. There is a clear correlation between the experimentally observed ion fractions and the lateral variation of the electrostatic potential on the surfaces. This correlation is believed to be caused by the variations in surface to atom electron transfer rates due to tunneling barriers introduced by the electrostatic potential on the surfaces.

This work was supported in part by the MRSEC Program of the National Science Foundation under Award No. DMR-9632667 and by the National Science Foundation Grant No. DMR-9521444.

-
- [1] B.H. Cooper and E.R. Behringer, in *Low Energy Ion Surface Interactions*, edited by J.W. Rabalais (Wiley, New York, 1994), pp. 263–312.
 - [2] J.P. Gauyacq and A.G. Borisov, *J. Phys. Condens. Matter* **10**, 6585 (1998).
 - [3] K.A.K. German, C.B. Weare, P.R. Varekamp, J.N. Andersen, and J.A. Yarmoff, *Phys. Rev. Lett.* **70**, 3510 (1993).
 - [4] P. Nordlander and J.C. Tully, *Phys. Rev. B* **42**, 5564 (1990).
 - [5] A.G. Borisov, D. Teillet-Billy, and J.P. Gauyacq, *Phys. Rev. Lett.* **68**, 2842 (1992).
 - [6] H. Shao, P. Nordlander, and D.C. Langreth, *Phys. Rev. B* **52**, 2988 (1995).
 - [7] J.B. Marston, D.R. Andersson, E.R. Behringer, and B.H. Cooper, *Phys. Rev. B* **48**, 7809 (1993).
 - [8] N. Lorente and R. Monreal, *Phys. Rev. B* **53**, 3303 (1996).
 - [9] A.G. Borisov, V. Sidis, and H. Winter, *Phys. Rev. Lett.* **77**, 1893 (1994).
 - [10] O. Grizzi, M. Shi, H. Bu, and J.W. Rabalais, *Rev. Sci. Instrum.* **61**, 740 (1990).
 - [11] C.C. Hsu, A. Boussetta, J.W. Rabalais, and P. Nordlander, *Phys. Rev. B* **47**, 2369 (1993).
 - [12] J. Ahn and J.W. Rabalais, *J. Phys. Chem. B* **102**, 223 (1998).
 - [13] J.W. Rabalais, *CRC Crit. Rev. Solid State Mater. Sci.* **14**, 319 (1988).
 - [14] V. Bykov, C. Kim, M.M. Sung, K.J. Boyd, S.S. Todorov, and J.W. Rabalais, *Nucl. Instrum. Methods Phys. Res., Sect. B* **114**, 371 (1996).
 - [15] J. Mackey, L. Lou, and P. Nordlander, *J. Chem. Phys.* **102**, 7484 (1995).
 - [16] P. Nordlander and N.P. Lang, *Phys. Rev. B* **44**, 13 681 (1991); A.G. Borisov, G.E. Makhmetov, D. Teillet-Billy, and J.P. Gauyacq, *Surf. Sci.* **350**, L205 (1996).
 - [17] J.F. Zeigler, J.P. Biersack, and U. Littmark, *The Stopping and Range of Ions in Solids* (Pergamon, New York, 1985).
 - [18] D.C. Langreth and P. Nordlander, *Phys. Rev. B* **43**, 2541 (1991).